



A feasibility study of LoRaWAN-based wireless underground sensor networks for underground monitoring

Guozheng Zhao, Kaiqiang Lin, Tong Hao^{*}

College of Surveying and Geo-Informatics, Tongji University, Shanghai, China



ARTICLE INFO

Keywords:
LoRaWAN
Wireless underground sensor networks
Underground monitoring
Physical layer parameters

ABSTRACT

With the continuous expansion of human interaction with the underground space, the observation of underground environment (e.g. soil moisture) and underground infrastructure (e.g. underground pipelines), as well as the monitoring and prevention of geological disasters (e.g., landslide and urban sinkholes) has attracted increasing attention and become a research focus. However, most of the traditional observation technologies are still facing difficulties in dynamic and continuous *in-situ* observations/monitoring within the complex underground environment. To solve this problem, this study adopts LoRaWAN-based wireless underground sensor networks (WUSNs) to monitor the underground environment or infrastructure. Furthermore, the feasibility of LoRaWAN-based WUSNs for underground monitoring is systematically demonstrated and presented in this article. Based on our recent validation of LoRa-based underground point-to-point channel model, we evaluate its network-level performance in this paper. We firstly develop a network simulator of LoRaWAN-based WUSNs to provide the feasibility analysis and experimental guidance for underground monitoring. Using this simulator, we numerically demonstrate that the LoRaWAN-based WUSNs technology is capable of underground monitoring over a large area and at great depths. We further certify that an appropriate selection of the physical layer parameters in various underground conditions is beneficial for underground observation. Finally, the balance between data receiver rate and network energy consumption can be implemented using different physical layer parameters for various underground monitoring applications. These results successfully demonstrate the efficient protocol development of LoRaWAN-based WUSNs and their applicability for underground monitoring applications.

1. Introduction

As the exploitation and development of underground space continue to grow, monitoring and assessment of the underground environment and underground infrastructure have attracted a lot of attention [1], with traditional *in-situ* ground survey and airborne observation starting to expand to the underground domain. Traditional Earth observations are normally aided by remote sensing technologies for the observations of systematic changes of targets [2], and these observations are generally macroscopic with a large surveying span, and cannot continuously monitor the dynamic changes of the targets [3,4]. On the other hand, the geophysical technologies, taking ground penetrating radar as an example, provide *in-situ* detection of the subsurface targets. However, they are not continuous measurements, thus long-term monitoring is infeasible. To fill these gaps, researches have proposed the wireless underground sensor networks (WUSNs) technology, enabling the

monitoring of underground targets [5] in a long-term and *in-situ* manner. Wireless underground sensor networks (WUSNs), as the natural extension of WSNs to the underground domain, install multiple subsurface sensors to gather the information about underground environment and the sensing data are transmitted to the gateways on the ground surface (see Fig. 1). They can ensure continual, real-time monitoring of the underground and are designed for various applications [5–7], such as condition assessment for underground infrastructure, environmental disaster monitoring and soil properties monitoring for precision agriculture. However, the direct adoption of the traditional WUSNs for subsurface monitoring is not preferable, since they are not conducive to long-term underground monitoring over long distances. Firstly, due to the complex underground environmental influencers such as soil properties, density, and volumetric water content (VWC), traditional wireless communication technologies could not support long-distance underground communications [8,9]. Furthermore, the energy consumption of

* Corresponding author.

E-mail address: tonghao@tongji.edu.cn (T. Hao).



Fig. 1. Applications of WUSNs.

battery-powered nodes deployed underground is also a drawback for WUSNs implementation [5,10]. These disadvantages make conventional WUSNs unsuitable for large scale underground Earth observations. To tackle this problem, long-range and low-power wireless communication technologies have been proposed and developed for WUSNs in recent years [11–13].

The low-power and long-range propagation characteristics of the Low-Power Wide-Area Networks (LPWANs) technology can be tailored for WUSNs. At present, LPWANs technologies include the Long Range (LoRa), the Narrowband-IoT (NB-IoT), and the Sigfox, etc. [14]. In particular, LoRa offers arguably a better security, higher maximum packet length, unlimited number of transmission messages per day, and support for deployment of a private Long-Range Wide Area Network (LoRaWAN) [12]. These elements make LoRa a promisingly suitable candidate for WUSNs, and hence we focus on the combination of LoRaWAN and WUSNs in this study.

Although the propagation characteristics and the link quality for point-to-point transmission in WUSNs have been investigated [15–17], the feasibility studies of adopting LoRaWAN-based WUSNs for underground monitoring at the network level are essential, and serve as one of our motivations. Considering the difficulty of deploying large-scale underground nodes, we develop a network simulator to evaluate the network performance and provide a simulation experimental guidance for underground applications. In this simulator, we adopt LoRa as the physical layer and LoRaWAN as the MAC layer. Furthermore, in this feasibility study, we quantify the network performance with three factors, i.e., the data extraction rate (DER), the goodput at a gateway and the energy per packet (EPP). We approach this feasibility study from three perspectives i.e., the underground environmental conditions, the capacity and scalability of LoRaWAN-based WUSNs, and the optimum adoption of the physical layer parameters. On the whole, our motivation is to explore the feasibility of LoRaWAN-based WUSNs for underground monitoring by evaluating their performance at the network level with simulation experiments.

The main contributions of the paper can be summarized as follows:

- 1) We develop an underground-aboveground network-level simulator of LoRaWAN-based WUSNs based on LoRaSim [18] to mimic the process of signal propagation through the complex underground domain. This simulator considers the bi-directional transmission between nodes and a gateway with the communication protocol LoRaWAN, as well as the underground conditions, by using the state-of-the-art channel models for WUSNs.
- 2) We quantitatively verify the feasibility of LoRaWAN-based WUSNs for underground monitoring through the network performance evaluation. We discover that LoRaWAN-based WUSNs enable deeper and wider underground monitoring with good network performance compared to traditional WUSNs.
- 3) We evaluate the impact of the underground environment, network scale and physical layer parameters on the network performance, which can provide theoretical and numerical guidance for future practical applications.
- 4) We quantitatively investigate how the underground environment complicates the adjustment of physical layer parameters to the

network performance. Hence, we herein suggest to consider the effects of different subsurface environments when adjusting the physical layer parameters to further improve the depth and breadth of underground monitoring applications.

The rest of this paper is organized as follows. Section 2 reviews the works related to LoRaWAN-based WUSNs. In Section 3, the technology overview of LoRa and LoRaWAN is presented. The simulation framework and design developed in this study are introduced in Section 4. The impacts of the underground environmental conditions, the network capacity and scalability, and the physical layer parameters on the performance of underground monitoring are numerically evaluated in Section 5. Finally, conclusions are drawn in Section 6.

2. Related works

Recently, the wireless underground communications have been widely investigated. In [19], the theoretical channel models of the communications between underground and aboveground nodes were developed, which laid the theoretical foundation for the study of underground-aboveground wireless communications. Besides these theoretical models, the experimental results in [20] verified that the maximum communication distance is 7 m at the burial depth of 0.4 m when soil's VWC is 10.85%. The experimental results revealed that the traditional wireless communication technologies cannot support the large scale WUSNs deployment. More recently, with the development of LPWANs technologies such as LoRa, the authors in [17] experimentally evaluated the LoRa propagation characteristics in soils for WUSNs in terms of the packet success rate. They concluded that VWC, burial depth and LoRa payload significantly impact the LoRa propagation characteristics. In 2019, we further experimentally verified the impact of the LoRa's physical layer parameters on the link quality under different underground environmental conditions [13]. Although these insightful works were focused on LoRa-based WUSNs, they were point-to-point studies, i.e., a node deployed in soil transmits/receives a packet to/from an aboveground gateway. To our best knowledge, there have been no studies on the feasibility of underground monitoring by adopting LoRaWAN-based technology.

Before moving into the network level of WUSNs, it is necessary to review the related works on the traditional aboveground LoRaWAN. Currently, there are many studies of the LoRaWAN performance by using mathematical analysis [21], simulation experiments [22] and field measurements [23]. In [24], the capacity and scalability analysis of the LoRaWAN was presented. Although this work preliminarily studied the network performance of LPWAN technology, it utilized the networking design as the pure ALOHA protocol, in which the capture effect and the effects of interference needs to be further investigated. In order to be more aligned with the realistic applications, the authors in [25] analyzed the scalability of large-scale LoRaWAN networks by applying the interference model in the LoRa error model, which was incorporated in the ns-3 model. Their results illustrated that a gateway (GW) may communicate with tens of thousands of end nodes (EDs) and the capacity of the uplink channel depends largely on the distance between the ED and the GW. Furthermore, a thorough study of LoRaWAN performance was presented in [26], where their simulation results showed that a reasonable setting of the system parameters can significantly improve the LoRaWAN performance. In addition, the author in [27] evaluated the influence of the physical layer parameters on the LoRaWAN, which demonstrated that by choosing the optimal BW and SF it is feasible to improve the LoRaWAN network performance. We summarize several related works in Table 1, which is by no means complete but only for representative purposes.

Table 1
Summary of related works.

Technology area	Authors & Year	Study purpose	Study type	Main findings / conclusions
WUSNs	Sun et al. [19], 2011	Develop a mathematical model to analyze the dynamic connectivity in WUSNs	Mathematical analysis	Based on the propagation medium, three different channel models were constructed. Analyzed the effects of different systems and environmental parameters on WUSN connectivity.
	Silva et al. [20], 2015	Explore the link quality properties of the three communication channels used in WUSNs for underground pipeline monitoring by experimental study	Field measurements	The channel links in UG2AG are stable but with limited communication range. UG2AG and AG2UG channels are sensitive to changing soil conditions and limited by communication range.
	Wan et al. [17], 2017	Evaluate the LoRa propagation characteristics in soils for WUSNs.	Field measurements	VWC, burial depth and LoRa payload significantly impact the LoRa propagation characteristics.
	Lin et al. [13], 2019	Study the UG2AG link quality in LoRa-based WUSNs	Field measurements	LoRa technology has good capability in underground environments and can effectively deal with the problem of limited communication range of UG2AG channels.
LoRaWAN	Mikhaylov et al. [24], 2016	Analyze the capacity and scalability of LoRaWAN with a single base station	Simulation experiments	A single base station can cover millions of devices. The uplink channel capacity of a node heavily relies on the distance from the base station.
	Abeeel et al. [25], 2017	Explore the scalability of large-scale LoRaWAN networks	Simulation experiments	A gateway may communicate with tens of thousands of end nodes. It is important for the LoRaWAN performance to assign network parameters to end nodes.
	Bouras et al. [27], 2018	Evaluate the influence of the physical layer parameters on the LoRaWAN	Simulation experiments	It is feasible to improve the LoRaWAN network performance by choosing the optimal BW and SF.
	Magrin et al. [26], 2019	Study the impact of different network parameters on the LoRaWAN performance	Simulation experiments	A reasonable setting of the system parameters can significantly improve the LoRaWAN performance.

3. Technology overview

3.1. LoRa

LoRa is a Chirp Spread Spectrum (CSS) modulation technique developed by Semtech Corporation [28], which employs an up-chirp base symbol. LoRa is designed to transmit information wirelessly at long-distance and with low power. However, the transmission range and the energy consumption of LoRa depend on multiple communication parameters, i.e., Transmit power (TP), Spreading Factor (SF), Coding Rate (CR), and Bandwidth (BW). Higher TP improves the received signal quality and expands the communication range at the cost of the increase in the energy consumption at end devices. Considering that SF ranges from 7 to 12, the higher value of SF, the longer the propagation distance, with the corresponding lower transmission rate and prolonged time-on-air (ToA). On the other hand, CR, the proportion of the useful parts of the data stream, can increase the robustness to interference. Furthermore, one can improve the reliability and the range of Lora by adopting Forward Error Correction (FEC). BW refers to the width of the frequency band occupied by the signals, which are normally 125, 250, or 500 KHz. A higher channel bandwidth allows higher data rates with shorter ToA, but it limits the propagation distance.

3.2. LoRaWAN

LoRaWAN is a communication protocol and system architecture designed for LoRa networks, which is officially defined by the LoRa

Alliance [29]. Unlike the physical layer protocol, LoRaWAN is a cloud-based Medium Access Control (MAC) layer protocol. Fig. 2 illustrates a typical LoRaWAN architecture, which normally consists of nodes or end devices (EDs), gateways (GWs), and network servers (NSs). It commonly uses the star topology to connect the multiple EDs with one GW or multiple GWs.

In a typical LoRaWAN, there are three classes of EDs: Class A, B, and C, corresponding to different capabilities of the devices. Class A devices receive downlink packets by opening the receiving window immediately after finishing the uplink transmission. Different from Class A, Class B devices open the receiving window at a specified time to receive downlink data. Class C devices open the receiving window continuously to listen to the downlink data traffic. Among these three classes of EDs, Class A devices consume the lowest energy due to the shortest timing of the receiving window. Therefore, we only focus on Class-A EDs in the current study. Fig. 3 illustrates the downlink receiving window timing for Class A devices. In this process, an ED that needs acknowledgement (ACK) packets should open RX1 and check whether a physical layer preamble has been received after opening the receiving window. If a preamble has been detected, the ED will continue to receive the downlink data transmission. When an ED receives the downlink data in the first receiving window, it is not essential to open the second receiving window. Otherwise, it must open the second window (RX2) one second after opening the first window. If an ED successfully receives a downlink packet in RX1 or RX2, it will enter an idle state. If not, the ED needs to re-transmit the uplink packet until the ACK packets are received or the maximum number of re-transmissions is reached. If an ED eventually could not receive any ACK packets, it means the GW fails to receive the packet. Note that in China, the uplink and downlink do not use the same frequency band, for example, the frequency band of uplink is CN470, the frequency band of downlink is CN510. Hence the ED listens on a channel that is different from the last uplink transmission in the receiving window. Although the frequency bands of uplink and downlink are different, SF keeps the same in the uplink and downlink.

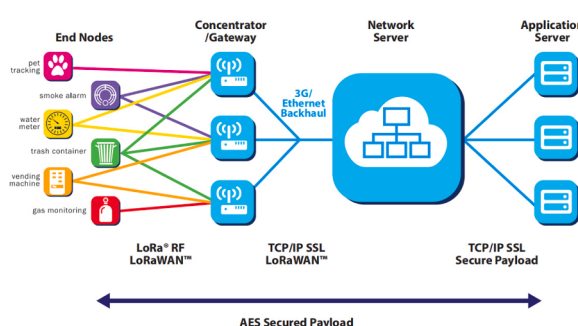


Fig. 2. Network architecture of LoRaWAN (courtesy of Semtech).

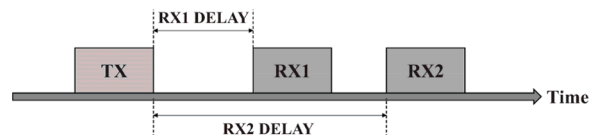


Fig. 3. Timing of the receiving windows for Class A EDs.

4. Simulation platform

One of the most popular simulators for LoRaWAN is LoRaSim [18], which is a discrete-event simulator based on Python with a SimPy simulation library. However, this simulator does not include the underground simulation and enable bi-directional transmission between nodes and a gateway. Moreover, the MAC layer behaviours (e.g. duty cycle) are not implemented. In this study, we develop a simulator based on Python with a SimPy simulation library to provide a feasibility analysis of underground monitoring by evaluating the LoRaWAN-based WUSNs performance. This simulator fills the gaps in LoRaSim and enables two-way communication from underground to aboveground, which is essentially tailored for underground monitoring applications.

In this section, we describe this simulation platform in detail. The channel models for generic WUSNs are firstly presented, followed by our developed LoRaWAN-based WUSNs architecture. The simulator system architecture is then introduced, before three key evaluation metrics are deduced in detail.

4.1. Channel models for WUSNs

Proper channel models for electromagnetic (EM) wave propagation in air and soil serve as the basis of WUSNs. In [19], the authors proposed a novel path loss model for UG2AG and AG2UG communications, which is the classical channel model for WUSNs. However, this work has not yet considered the attenuation caused by lateral waves in UG2AG/AG2UG communications. This attenuation must not be ignored especially when the receiver is placed in the vicinity of the ground surface. The authors in [30] took into account this part of attenuation that caused by lateral waves and validated the accuracy of the model by carrying out field experiments. Hence, in this paper, we take advantage of the channel models in [16,30] for the underground-to-aboveground (UG2AG) and aboveground-to-underground (AG2UG) communications, which are illustrated in Fig. 4. The burial depth (Depth) of an ED is h_u , the height of a GW deployed above the ground surface is h_a , d_{ug} is the distance of the underground communication, d_{ag} is the distance of the aboveground communication, $d_{internode}$ is the horizontal distance between a GW and an ED, and $d_{surface}$ is the distance accounting for the soil-air interface propagation.

The received signal strength, P_r , at the receiver is given by:

$$P_r = P_t + G_t + G_r - \left[L_{ug}(d_{ug}) + aL_{ag}(d_{ag}) + bL_{surface}(d_{surface}) + L_R - 10\log\chi^2 \right] \quad (1)$$

where P_t is the transmitted power, G_t is the transmitter antenna gain, G_r is the receiver antenna gain, $L_{ug}(d_{ug})$ and $L_{ag}(d_{ag})$ are the path losses in soils and air, respectively. $L_{surface}(d_{surface})$ is the attenuation caused by lateral waves, L_R is the refraction loss, $-10\log\chi^2$ is the attenuation caused by the multipath fading. a and b in (1) are the coefficients of L_{ag} and $L_{surface}$, respectively. In this study, due to the nodes are not in

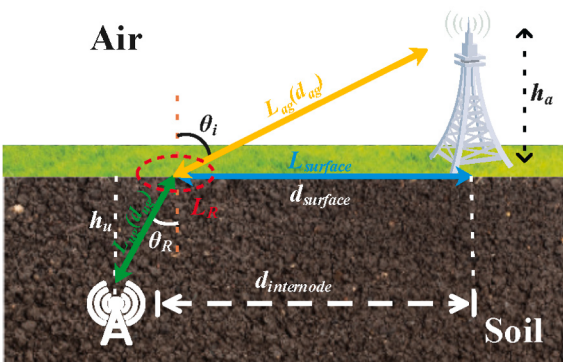


Fig. 4. The channel models of UG2AG and AG2UG communications.

proximity to the soil-air interface, and the GW is placed 3 m above the ground surface, the attenuation of lateral waves can be ignored [31], we set a equals 1 and b equals 0. χ is a random variable of the Rayleigh distribution and the probability density function of χ is:

$$f(\chi) = \frac{\chi}{\sigma_R^2} e^{-\chi^2/\sigma_R^2} \quad (2)$$

where σ_R is Rayleigh distribution parameter.

In (1), $L_{ug}(d_{ug})$ and $L_{ag}(d_{ag})$ can be calculated by:

$$L_{ug}(d_{ug}) = 6.4 + 20\log d_{ug} + 20\log \beta + 8.69\alpha d_{ug} \quad (3)$$

$$L_{ag}(d_{ag}) = -147.6 + 20\log d_{ag} + 20\log f \quad (4)$$

where f is the operation wave frequency, α and β are the attenuation constant and the phase shifting constant, which are given as:

$$\alpha = (2\pi c / \lambda_0) \sqrt{(\mu_r \mu_0 \epsilon' \epsilon_0 / 2) \left[\sqrt{1 + (\epsilon''/\epsilon')^2} - 1 \right]} \quad (5)$$

$$\beta = (2\pi c / \lambda_0) \sqrt{(\mu_r \mu_0 \epsilon' \epsilon_0 / 2) \left[\sqrt{1 + (\epsilon''/\epsilon')^2} + 1 \right]} \quad (6)$$

where ϵ' and ϵ'' are the real part and imaginary part of the soil's dielectric constant, respectively [32].

In the UG2AG communication, the refraction losses, L_R in (1), can be given by:

$$L_R = L_{ug-ag} \simeq 10\log \left[(\sqrt{\epsilon'} + 1)^2 / 4\sqrt{\epsilon'} \right] \quad (7)$$

Correspondingly, L_R for the AG2UG communication is written as:

$$L_R = L_{ag-ug} \simeq 10\log \frac{(\cos\theta_I + \sqrt{\epsilon' - \sin^2\theta_I})^2}{4\cos\theta_I\sqrt{\epsilon' - \sin^2\theta_I}} \quad (8)$$

where θ_I is incident angle [33].

4.2. Simulation process of lorawan-based WUSNs

We now design the simulation process of how an ED sends a packet to a GW, whose flowchart is illustrated in Fig. 5. Firstly, it is essential to set initial parameters. Before the uplink transmission is initiated, the EDs need to be deployed randomly. When the packets are transmitted to a GW, it will check if there are any packet losses and packet collisions. Once the signal strength received by the GW exceeds the receiver sensitivity and no collisions occurring between packets, the packets can be received by the GW. Furthermore, the packet is checked at the GW whether ACK is needed. If the packet requires ACK, the GW attempts to perform the downlink transmission. If the packet does not demand ACK, the simulation will end. To better understand the simulation process, the physical layer and MAC layer parameters are illustrated as follows.

- In order to complete the WUSNs simulation based on LoRaWAN, multiple EDs are randomly deployed in soils, and the physical layer

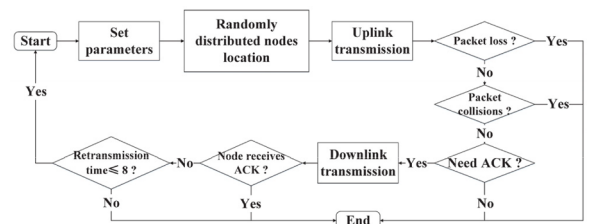


Fig. 5. The flowchart of the LoRaWAN-based WUSNs simulator.

Table 2
Sensitivity of LoRa (in dB).

BW\SF	7	8	9	10	11	12
125 kHz	-126.50	-127.25	-131.25	-132.75	-134.5	-137.25
250 kHz	-124.25	-126.75	-128.25	-130.25	-132.75	-134.00
500 kHz	-120.75	-124.00	-127.50	-128.75	-128.75	-132.25

parameters, i.e., TP, SF, BW, CR, are set. Furthermore, considering the receiver sensitivity is mostly affected by SF and BW, the receiving sensitivities of LoRa with different SF and BW are shown in Table 2.

- LoRaWAN MAC layer enables EDs to communicate with GWs and provides the network protocol to monitor transmission status. Considering the upstream transmission, there are eight channels for EDs to transmit data. However, the transmission is affected by the duty cycle regulations, e.g., 0.1%, 1% and 10%. If an ED has transmitted packets over a channel, other EDs cannot transmit packets over the same channel in a duty cycle. The duration of the pause time, T_{off} , can be calculated by:

$$T_{off} = (T_{air} / \text{Duty Cycle}) - T_{air} \quad (9)$$

where T_{air} is the air time of a packet, and *Duty Cycle* is the local duty cycle. Similar to the uplink transmission, the downlink transmission has eight available channels which is also affected by such duty cycle restriction.

4.3. Network architecture

In this section, we present the implementation details of our LoRaWAN-based WUSNs simulator. We illustrate the network architecture which includes the physical layer, MAC layer, data transport layer and application layer, as displayed in Fig. 6. In this network architecture, the network layer is not necessary and excluded because the nodes are directly connected to a gateway, therefore the route planning is not involved in this simulator. The details of the network architecture are as follows.

4.3.1. Physical layer

4.3.1.1. *Physical layer for nodes*. The communications between nodes

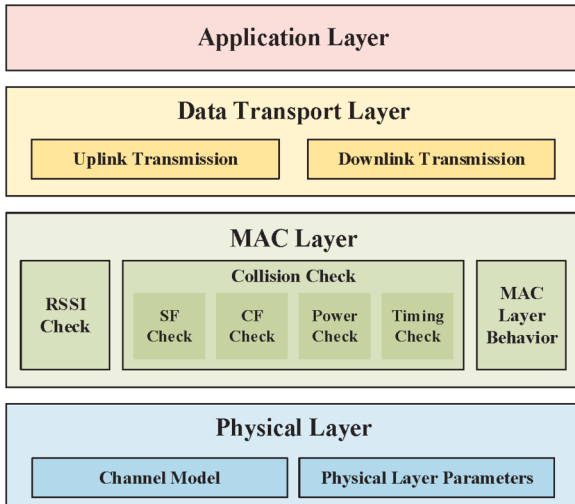


Fig. 6. Network architecture.

and a gateway may use different data rates and frequency channels. For LoRa, there are different physical layer parameters to be selected or optimized for various purposes, as stated in subSection 3.1. Four key physical layer parameters, i.e., TP, SF, BW, CR, are set at each node, according to the practical needs. Whether the packet is received or not will be further verified by the MAC layer of a gateway.

4.3.1.2. Physical layer for gateway. Unlike the physical layer for nodes, a gateway transmits packets to all nodes with the same physical layer parameters (in this study: TP = 14 dBm, SF = 12, CR = 4/8 and BW = 125 kHz) to make sure the packets reach the corresponding node. Furthermore, there are different frequency bands between the uplink and downlink due to the CN470–510 standard, where 80–87 bands for the CN470 and CN510 are selected for the uplink and downlink transmissions, respectively. The calculation of the path loss for packet transmission is based on the channel models introduced in subSection 4.1. Besides, we set a list to reserve the information of packets arriving at the gateway, which is used for checking the collision between packets. Such checks are implemented at the MAC layer of the gateway.

4.3.2. MAC layer

4.3.2.3. MAC layer for nodes. Checking of a free channel is necessary before a node sends packets. This check should comply with the duty cycle regulation, which has been described in subSection 4.2. A node can only send a packet if there are free channels, otherwise the node must wait. After a channel finishing transmitting a packet, its state will be stored in a defined variable *ProhibitedUSE*. It can only be changed to *PermissionUSE* when T_{off} has elapsed, see (9) in subSection 4.2.

In addition, if a packet needs an ACK, the node should open the receiving windows to receive the downlink packets from the gateway, as described in subSection 3.2. If the node does not receive the packet from the gateway, it needs to retransmit the packets to the gateway. Furthermore, we set a variable *NumberRetransmit* to record the number of retransmissions and give up transmitting packets if *NumberRetransmit* > 8.

4.3.2.4. MAC layer for gateway. When a packet arrives at the gateway, its RSSI at the gateway can be calculated by (1). Only when this RSSI is higher than the sensitivity (Table 2) do we continue to check the collision. Conversely, we can directly record that this packet is lost. If the packet is confirmed not lost, the collision checking between packets must be performed [18]. As mentioned in 4.3.1, the gateway has a list to reserve the information of the packets arriving at the gateway. In this information list, we reserve the classes corresponding to nodes, which includes SF, Carrier Frequency (CF) and RSSI. According to *env.time* in Simpy simulation library [18], we can obtain the time of packet arrival at the gateway, and identify whether two LoRa transmitted packets x and y overlap at the gateway. The reception interval for a packet i can be defined as (a_i, b_i) , with the midpoint $m_i = (a_i + b_i)/2$ and the midpoint length $d_i = (b_i - a_i)/2$. If $|m_x - m_y| < d_x + d_y$, these two packets overlap. After this, we need to check if they are colliding, using *frequencyCollision*, *sfCollision*, *powerCollision* and *timingCollision* functions in the simulator.

First, if two packets x and y have the same SF, *SFCollision* is true. Second, we determine whether they have the same CF by comparing the values of $|f_x - f_y|$ and $f_{threshold}$. If $|f_x - f_y| < f_{threshold}$, it means that they have the same center frequency. Here, f_x and f_y are the center frequencies of packet x and y , respectively. $f_{threshold}$ is the defined tolerable frequency offset, which relies on the bandwidth [18]. Third, if packets x and y arrive at the gateway with a small RSSI difference, they may be collided, and one needs to check the condition $|RSSI_x - RSSI_y| < P_{threshold}$, and if it is true, they are collided. Only the one with the bigger RSSI can be captured. In this simulation, $P_{threshold}$ is set to 6 dBm. According to [18], we know that it is permissible to lose ($N_{preamble} - 5$) preamble symbols at

most. Therefore, the interval for the transmitted packet x is redefined as $(a_x + T_{sym} \cdot (N_{pream} - 5), b_x)$ and is judged whether to overlap or not. Only if these checks occur simultaneously can the two packets collide.

On the other hand, the MAC layer for the gateway needs to determine whether the received packet needs an ACK, which is defined in our simulator as *RequireACK*. A packet requiring ACK means that the gateway should transmit data to the corresponding node. Instead, no downlink packets need to be sent.

4.3.3. Data transport layer and application layer

The data transport layer focuses on the interactions between nodes and a gateway. It includes both the uplink and downlink transmissions. All nodes send packets to the gateway through the uplink transmission. If packets from a node need ACK, the gateway should transmit it to the corresponding node through the downlink transmission.

The application layer includes a set of simulation parameters including the size of packets sent by nodes, the transmission time interval, the number of nodes, the deployment radius and the burial depth of nodes, etc.

4.4. Network environment

The network environment of the LoRaWAN-based WUSN includes the physical environment and the logical environment. In the physical environment, the network consists of a gateway and multiple nodes. The gateway is placed 3 m above the ground. Moreover, the aboveground environment is set with no obstacles by any infrastructure to ensure line-of-sight communications. The nodes are deployed underground to monitor the underground conditions. The underground soil composition and soil properties are shown in Table 3, and the description of the network deployment parameters is provided in Table 4. In the logical environment, the LoRaWAN-based WUSN uses the stars topology, as illustrated in Fig. 7, in which all nodes are directly connected to a gateway, and this network topology communicates according to the LoRaWAN communication protocol [29].

4.5. Evaluation metrics

For a WUSN, it is significant only if the packets sent by the underground nodes are successfully received by a gateway. Therefore, the data extraction rate (DER) is an essential evaluation metric. The throughput is usually used to indicate whether the packet being sent has arrived correctly in a network. Goodput is the same as throughput except that it measures the speed of data from node to gateway. We adopt goodput as one of the evaluation metrics. Considering the nodes are buried underground, the network energy consumption is a vital factor. We shall reduce energy consumption as much as possible while maintaining DER. For the above considerations, the energy per packet (EPP) becomes another evaluation metric of the LoRaWAN-based WUSNs. The detailed instruction of three key network-level metrics is as follows.

Goodput at a GW is defined as:

$$\text{Goodput} = \frac{N_{arrived} \times PL}{T_{simulation}} = \text{DER}_{\text{upstream}} \times PL \times \frac{N_{transmitted}}{T_{simulation}} \quad (10)$$

where $N_{arrived}$ is the number of packets arrived at a GW, PL is the packet length in bytes, $T_{simulation}$ is the duration of a simulation, $\text{DER}_{\text{upstream}}$ is the

Table 4
Default values of parameters in simulation.

Parameters	Value
Number of Nodes	100
Communication Radius	50 m
Gateway Height	3 m
Simulation Time	30 days
Burial Depth	0.1 m
Volumetric Water Content	10%
transmission rate	20 bytes per 30 min
center frequency	cn470–510 (80–87 bands)
Duty Cycle	1%
Spreading Factor (SF)	12
Transmission Power (TP)	14 dBm
Code Rate (CR)	4/8
Bandwidth (BW)	125 kHz

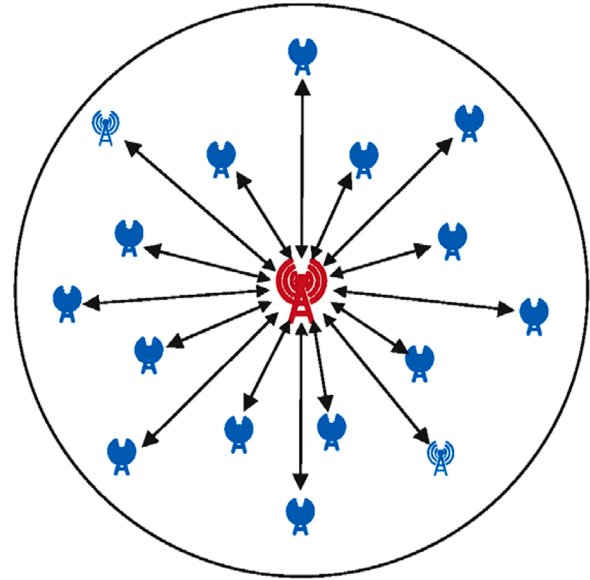


Fig. 7. The deployment and connection structure of nodes (in blue) and a gateway (in red).

data extraction rate with only upstream transmission. In this study, we only calculate the goodput at a GW.

DER can be given by [18]:

$$\text{DER} = N_{received} / N_{transmitted} \quad (11)$$

where $N_{received}$ is the number of packets received by a GW. If a packet is received, it means that both the upstream and downstream transmissions have been successful. $N_{transmitted}$ is the number of packets transmitted by the EDs.

EPP can be calculated by [34]:

$$\text{EPP} = \text{NEC} / \text{DER} \quad (12)$$

where NEC is the network energy consumption, which can be calculated as [35]:

$$\text{NEC} = N_{transmitted} \times (E_{transmission} + E_{processing}) \quad (13)$$

where $E_{transmission}$ is the energy consumption of transmissions, $E_{processing}$ is the energy consumption of data processing. $E_{processing}$ and $E_{transmission}$ can be given by:

$$E_{processing} = V_{supply} \cdot I_{work} \cdot T_{run} \quad (14)$$

Table 3
Soil composition and soil properties.

Soil texture	Sand	Clay	Silt	Particle density	Bulk density
Loam	40%	20%	40%	2.66 g/cm ³	1.5 g/cm ³

$$E_{transmission} = V_{supply} \cdot I_{transmitted} \cdot T_{transmitted} \quad (15)$$

where V_{supply} is the supply voltage and it is set at 3 V in this study, I_{work} is the working current, $I_{transmitted}$ is the transmission current. In this simulator, LoRa is implemented using the Semtech's SX1272 transceiver. I_{work} is set at 19.8 mA, while $I_{transmitted}$ depends on TP and is obtained in SX1272 LoRa Calculator [36] provided by Smetech. T_{run} is the program runtime and $T_{transmitted}$ is the duration of the transmission:

$$T_{transmitted} = T_{preamble} + T_{payload} \quad (16)$$

The preamble duration $T_{preamble}$ is given by:

$$T_{preamble} = (n_{preamble} + 4.25) \times 2^{SF} / BW \quad (17)$$

where $n_{preamble}$ is the number of preamble symbols, and $T_{payload}$ is the payload duration, which can be calculated as:

$$T_{payload} = \left(8 + \max \left(\text{ceil} \left(\frac{8PL - 4SF + 28 + 16 - 20H}{4(SF - 2DE)} \right) (CR + 4) \right) \right) \times 2^{SF} / BW \quad (18)$$

where H is used to identify whether the implicit header is disabled, which usually sets to 0 and sets to 1 only when SF=6 is employed. DE represents whether the data rate optimization is used. It is set to 1 when SF equals 11 or 12 and 0 when the rest of SF are employed.

5. Results and discussion

In this section, the influence of the different factors on the LoRaWAN-based WUSNs are presented through the simulation experiments by adopting the key evaluation metrics: goodput, DER, and EPP.

Although the point-to-point LoRa aboveground-underground communications have been investigated [13,17], the network performance cannot be a simple superposition of the performance of multiple EDs. This is because the EDs will undergo packet collisions, and suffer by the limitation of both the duty cycle and the channel number in the process of data packets transmission [22], which can largely affect the total network performance [25].

There are three main aspects to verify the performance of the LoRaWAN-based WUSNs.

- 1) Considering nodes are deployed underground, the influence of the underground environmental conditions on the network performance must be examined due to the strong effect of VWC and the burial depth on path losses;
- 2) For a network, the number of nodes represents the network's capacity to accommodate. The scope of a network represents the network's ability to expand. The larger the network, the better it is for extensive monitoring of the underground. Thus, the number and scope of EDs deployment which are the critical factors for environment monitoring applications also need to be discussed;
- 3) As we adopt LoRa technology, it is essential to discuss the impact of LoRa-specific physical layer parameters on the LoRaWAN-based WUSNs. Moreover, existing researches have confirmed that changing the physical layer parameters can improve the link quality of LoRa. We therefore study the impact of choosing different physical layer parameters for all nodes on the network performance. Besides these three main aspects, the impacts on the packet sending rate and the percentage of the number of EDs that need ACK packets to the total number of EDs are also examined.

In this work, considering the randomness of ED deployment and data transmission, the simulations were executed twenty times. Furthermore, goodput, DER, and EPP were calculated by using a median average filtering algorithm.

5.1. Initial parameters for the simulation

At the beginning of the simulation experiment, default parameters, such as the environment variables, the physical layer parameters and the MAC layer parameters need to be set. If not otherwise specified, the simulation configurations remain the same as those listed below as well as those in Tables 3-4. The default soil moisture content is 10%, the burial depth is set to 0.1 m. A 20-byte packet is sent from each ED to a GW every 30 min and the simulation time is 30 days. The duty cycle during each transmission is 1%. The center frequency of each transmission is chosen from the CN470–510 frequency band used in China. In this study, the number of channels available for the uplink and downlink transmissions is set at 8. Table 3 lists the soil properties with the soil composition set as a typical soil suitable for most plants [37]. Table 4 illustrates the physical layer parameter configuration of the transmission, and provides the center frequency of each transmission. At the network level, the positions of the EDs and GW are required for an accurate evaluation of the network metrics. Fig. 7 illustrates the two-dimensional deployment topology of nodes and a gateway. In this stars topology, nodes are deployed randomly in a circle and the gateway is placed at the center of this circle, and all nodes are directly communicating with the gateway. In simulations, the radius of the circle area and the number of nodes are initially set to 50 m and 100. In addition, the gateway is placed at the center of this circle, 3 m above the ground surface.

5.2. The influence of underground environmental conditions on the network performance

Fig. 8 displays the DER at various burial depths from 0 to 3 m with VWC ranging from 0 to 50% and ACK equals 10%. One can see that, in general, LoRaWAN-based WUSNs can support the communication with underground nodes at deeper burial depth, compared to traditional WUSNs such as those in [33,34]. Even under harsh underground conditions (e.g., VWC=50%), DER can sustain 0.92 at the burial depth of around 0.75 m. Such depth is sufficient for the monitoring application of most shallowly buried urban pipelines. It shall be noted that the maximum DER is 0.92 (Fig. 8) instead of the theoretical maximum 1, owing to the duty cycle limitation. Moreover, VWC and burial depth have a profound impact on DER as displayed in Fig. 8. Since both VWC and burial depth are highly correlated to path losses and the signal attenuation, they have a profound impact on DER. For instance, DER remains at 0.92 with the burial depth from 0 to at least 3 m at VWC equals 5%. However, DER starts to drop after a critical burial depth

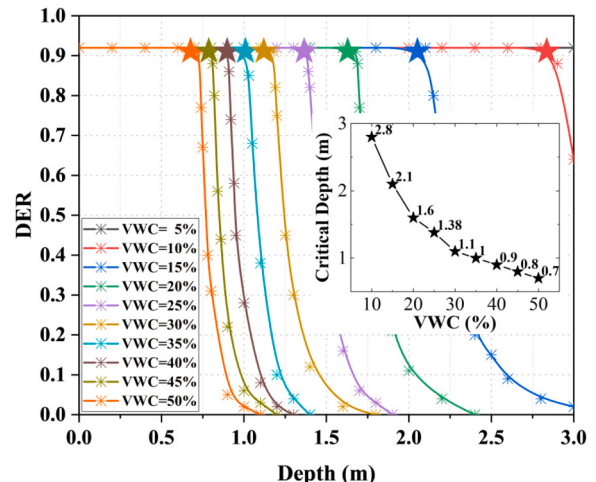


Fig. 8. The DER results with the change of burial depths and VWC.

(marked by the coloured star in Fig. 8), which is also dependent upon VWC. Such dependence is illustrated in the inset of Fig. 8. Furthermore, if the burial depth exceeds this critical value, DER will rapidly reduce to 0 with the increasing burial depth. The slope of such DER reduction is monotonically correlated to the increase of VWC. For instance, DER drops from 0.92 to 0 with the burial depth ranging from 1.6 to 2.4 m and 0.7 to 1.1 m, when VWC equals 20% and 50%, respectively. It is consistent with the result in [30], although the latter is the point-to-point communication.

The influence of the bidirectional traffic on LoRaWAN is always a topic that needs to be explored. The author in [38] illustrated the pros and cons of ACK for LoRaWAN aboveground. Considering the specificity of the underground environment and the infrequency of packets sent by the nodes, it is essential to examine the import of ACK on LoRaWAN-based WUSNs.

According to the LoRaWAN's criteria in the bidirectional communication, that the data are received by the gateway can be affirmed only if an ACK packet is received by the node. We can derive DER based on this rule. To verify the impact of ACK on DER, we randomly allocate SF ranging from 7 to 12, and the resultant effect is displayed in Table 5. We found that DER decreases with the increase in EDs that need ACK packets. According to the fact that DER equals to 0.92 when no EDs need ACK, it suggests that the decrease in DER is not caused by the path losses and the collision between data packets. Furthermore, the duty cycle limitation of the downlink transmission is not responsible for the decrease in DER because the number of EDs in the network is only 100 and each ED sends packets every 30 min on average. Based on the above inference, the main reason why DER decreases with the increased ACK packets may be that most of the time for the packets to reach the receiving window is less than 1 s due to the small SFs assigned to EDs. We conducted further simulations on the influence by varying SF and packet length (PL) on DER where ACK is required to EDs. The results show that a larger SF should be configured for a smaller PL, and a smaller SF for a larger PL. All the above investigation indirectly indicates that the use of ACK packets is not conducive to the LoRaWAN-based WUSNs. The main reason may be that most of the time for the packets to reach the receiving window is less than 1 s due to the small SFs assigned to EDs. Once the nodes do not receive the ACK packets, retransmission occurs. This excessively depletes the battery storage of the underground nodes. However, since battery power is a vital consideration for an underground node, it does not have to receive an ACK unless a bidirectional transmission is demanded in LoRaWAN-based WUSNs.

Although LoRa enables long-range and low-power transmission, it sacrifices transmission rate [39]. This is its downside. For underground monitoring applications, transmission rate represents the frequency of observations. Such transmission rate cannot be too high to save energy consumption, but it also cannot be too low since the environmental changes need to be accurately captured. Therefore, we study the impact of average transmission time interval (transmission rate) on the LoRaWAN-based WUSNs performance, as is shown in Fig. 9. It is observed that, in most underground environmental conditions, DER increases with the average time interval up to 60 mins, except for large VWC at large burial depths (e.g., VWC>30% and the Depth > 1.2 m), where the majority of packets are lost due to the path losses. In harsh underground environment (large VWC or Depth), transmission rate is not a critical factor compared to improving the link quality, thereby will not be considered. On the contrary with DER, the goodput drops sharply

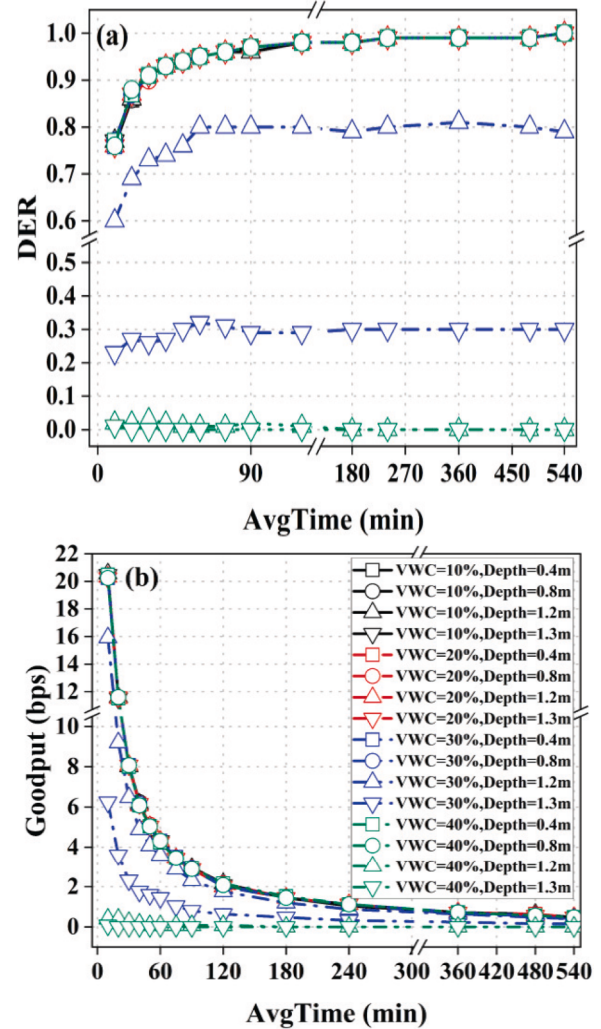


Fig. 9. (a) DER and (b) Goodput results with different average interval time.

with an average time interval from 10 to 120 min. For a network, larger DER and goodput are required. Thus, the average transmission time interval should not be less than 30 min in a good underground environment (e.g., VWC=10%, Depth=0.4 m). On the other hand, it should not be less than 60 min in a poor environment (e.g., VWC=30%, Depth=1.2 m).

5.3. The influence of the number and scope of nodes deployment on the network performance

Although LoRa officially claims a transmission distance of 20 km in air, this coverage may not apply to LoRaWAN-based WUSNs. In Fig. 10 (a), the impacts of the number of nodes and the deployment scope (e.g., radius) of the network on DER are displayed for a given underground condition, i.e., VWC=10%, Depth=0.1 m. The number of nodes ranges from 0 to 2000, with the deployment radius of the network ranges from 2 km to 20 km. Furthermore, ACK is set to 10% considering the downlink transmission. We can see that a gateway cannot cover the circle area of 1256 km² (transmission distance = 20 km) when nodes are buried underground. To ensure the good link quality (DER>0.8), a contour map (Fig. 11) is plotted, in which we can see that a gateway should have a coverage area of no more than 113 km² (transmission distance = 6 km), with the corresponding number of nodes being less than 1300. It should be emphasized that this result applies only for VWC equals to 10% and

Table 5
DER with the varying proportion of EDs that require ACK.

ACK (%)	0	10	20	30	40	50
DER	0.92	0.68	0.52	0.42	0.35	0.28
ACK (%)	60	70	80	90	100	
DER	0.26	0.21	0.18	0.17	0.15	

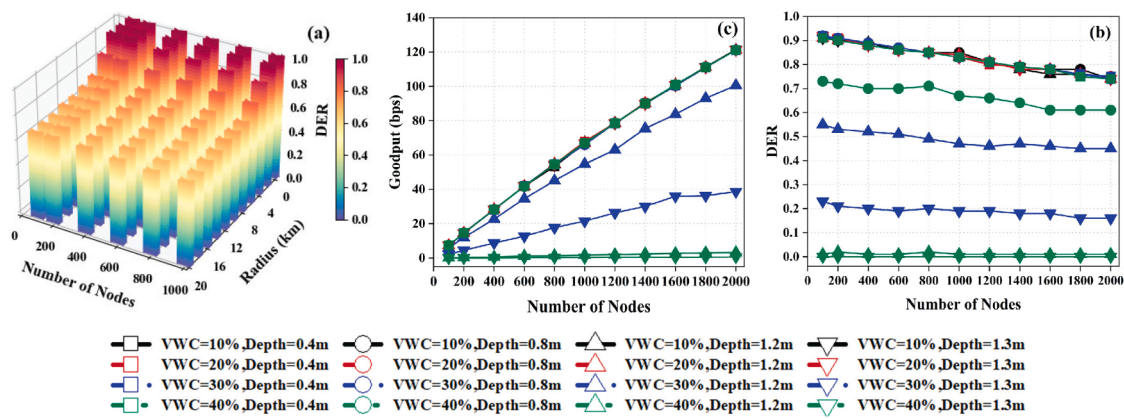


Fig. 10. Effects of network capacity and scalability on network performance. (a) DER with VWC=10% and depth=0.4 m. (b) DER, (c) Goodput at different underground environment.

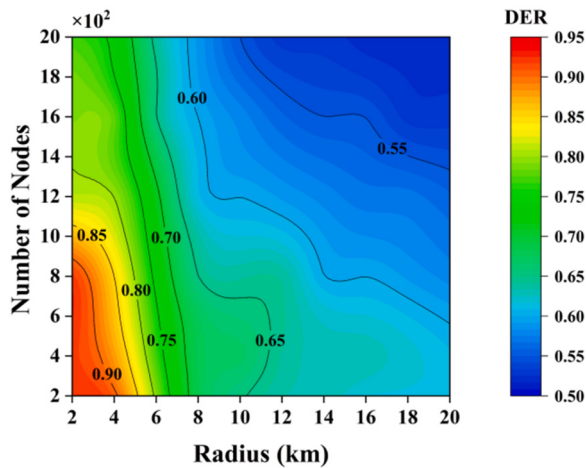


Fig. 11. The contour map of DER against the varying deployment radius and number of nodes (VWC=10% and Depth=0.1 m).

buried depth equals to 0.1 m. As displayed in Table 6, the coverage (radius) and number of nodes reduce with larger burial depths and higher VWC, due to the fact that the deeper and denser deployment of nodes increases path loss as well as the probability of collisions between packets. When the underground environment is poor, it is almost impossible to achieve a good link quality, which is consistent with Fig. 10(b). In this situation, it is unrealistic for the link quality greater

than 0.8. In some scenarios when the downlink transmission is not essential, one can simply set ACK=0, and the resultant limitation on the deployment scope and number of nodes are displayed in Table 7. It indicates that by avoiding the downlink transmission in harsh environments, it is feasible for greater coverage if DER > 0.8 is required.

Fig. 9(b) and (c) illustrate the influence of the number of nodes on DER and goodput for various underground environments. In Fig. 10(b), similar to the performance in air [41], DER decreases with the increasing number of nodes. It is also strongly correlated to the soil conditions, such as VWC and burial depth of the node. As illustrated in Fig. 10(c) and consistent with DER, the effect of the number of nodes on the goodput is mainly found in good and above underground environments. When the underground environment is poor or even harsh, this effect is small or even absent. In good underground environment, the goodput at a GW increases with the increasing number of nodes. Considering DER, a node count of 1300 is appropriate.

5.4. The influence of the physical layer parameters inside the lorawan on the network performance

Improving the accuracy of data reception and the network lifetime is particularly critical for real-time and continuous underground monitoring. The authors in [27] have demonstrated that different physical layer parameters have different degrees of influence on the network performance. Improper selection of physical layer parameters not only affects DER but also results in wasted energy. These results reveal that we need to look at the physical layer parameters to investigate these impacts on LoRaWAN-based WUSNs for more accurate data reception and longer network life. Therefore, we study the impact of the various

Table 6

The limitation of the deployment scope and number of nodes with ACK=10%.

VWC\Depth	0.4 m	0.8 m	1.2 m	1.3 m
10 %	(1800 m, 1300)	(720 m, 1300)	(390 m, 1300)	(320 m, 1300)
20 %	(850 m, 1300)	(250 m, 1300)	(95 m, 1300)	(72 m, 1300)
30 %	(480 m, 1300)	(100 m, 1300)	(46 m, 1300)	-
40 %	-	-	-	-

Table 7

The limitation of the deployment scope and number of nodes with no ACK.

VWC\Depth	0.4 m	0.8 m	1.2 m	1.3 m
10 %	(19 km, 1300)	(5.2 km, 1300)	(1.8 km, 1300)	(1.45 km, 1300)
20 %	(8.2 km, 1300)	(1.3 km, 1300)	(0.28 km, 1300)	(0.2 km, 1300)
30 %	(3.7 km, 1300)	(0.37 km, 1300)	(0.05 km, 1300)	-
40 %	(1.7 km, 1300)	(0.14 km, 1300)	-	-

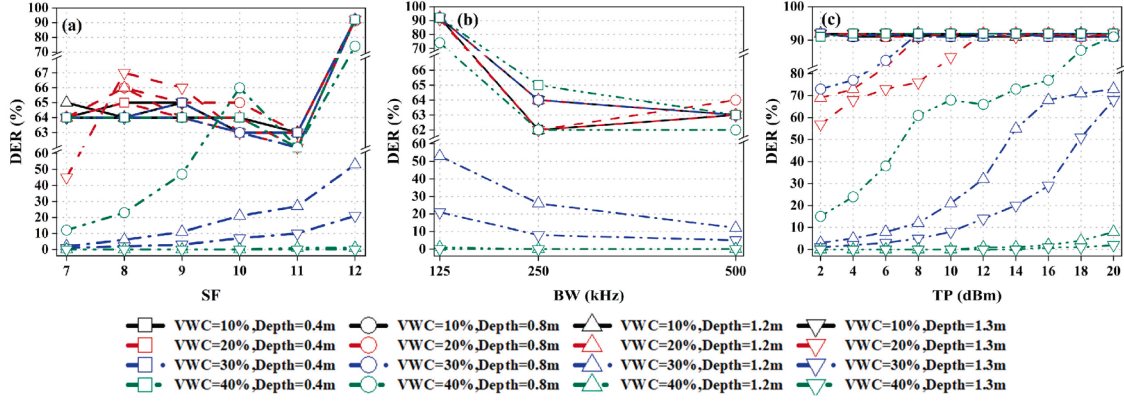


Fig. 12. Effects of (a) SF, (b) BW, (c) TP on DER for the different underground environments.

physical layer parameters such as SF, BW and TP on DER, the goodput at a GW, and energy under different underground environments. The corresponding results are displayed in Figs. 11–13. Moreover, we use the EPP [34] to verify the balance of DER and energy for different physical layer parameters, as illustrated in Fig. 15.

Fig. 12 shows the impact of the various physical layer parameters on DER under different underground environments (ACK=10%). In Fig. 12(a), when the deployment environment is good such as VWC=10% and Depth=0.4 m, DER always equals 0.64 with increasing SF ranging from 7 to 11, whereas DER reaches 0.92 when SF equals 12. The loss of packets mainly attributes to the loss of the ACK packets, which is because the airtime of the downlink transmission is so short that the receiving window cannot open in time to receive the ACK packets when SF is 7 to 11. However, no loss of the ACK packets owing to the increase in the airtime of the downlink transmission leads to the increase in DER when SF equals 12.

With the gradual deterioration of the underground environment, the loss of packets is mainly due to the path losses and the signal attenuation. Correspondingly, the grown in SF increases the link quality as well as the resultant higher communication reliability. For instance, DER increases from 0.02 to 0.53 as SF increases from 7 to 12 when VWC=30% and Depth=1.2 m. When the underground environment is very poor such as VWC=40% and Depth=1.2 m, the path losses and the signal attenuation are so large that the increase in SF could no longer help amplify DER at all.

Contrary to SF, the increase in BW leads to the reduction of DER under different underground environmental conditions in Fig. 12(b). However, the reasons for this reduction are different in various deployment environments. At the good underground environmental conditions, the increase in BW shortens the airtime of the downlink transmission, thereby the receiving windows don't open in time to

receive the ACK packets. However, the decrease in DER is mainly due to the path losses and the signal attenuation under the poor underground environmental conditions. In addition, the increase in BW leads to the increased receiving sensitivity, which in turn degrades the received signal quality, resulting in a further decrease in DER under the poor underground environmental conditions. Similar to SF, the environmental condition serves a more critical factor than BW for DER in challenging underground environments.

As shown in Fig. 12(c), the transmission power that equals 2 dBm leads to DER equals 0.92 for good deployment environments. It means that a small TP can meet the network requirement for dry and shallowly buried applications [40]. On the contrary, as in a poor underground environment, the increase in TP leads to an increased receiving power, which can overcome large path losses and signal attenuation and increase DER to a certain extent. For instance, DER reaches 0.92 at TP equals 20 dBm when VWC is 40% and Depth is 0.8 m. However, the path losses and the signal attenuation can be so significant that the increase in TP can no longer assure that the receiving power is greater than the receiving sensitivity, for certain harsh underground environments.

According to the above observation, different physical layer parameters used by all underground nodes have a significant impact on DER. Furthermore, these impacts are controlled by underground environments due to the geographical location where the nodes are randomly deployed. These results suggest that it is critical to consider the setting of physical layer parameters in the different underground environments for better DER (such as DER>0.8).

As shown in (10), when only uplink transmission is considered and other parameters remain constant, the goodput at the GW is mainly a function of DER_{uplink} . As a result, the goodput shall be positively correlated with DER of uplink transmission. In Fig. 13, we display the effect of the physical layer parameters on the goodput at a GW under different

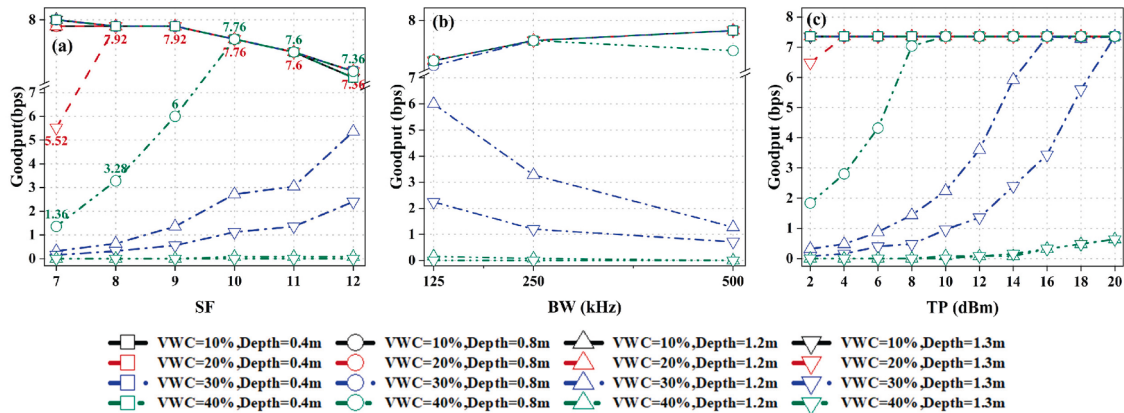


Fig. 13. Effects of (a) SF, (b) BW, (c) TP on the goodput for different underground environments.

underground conditions.

In Fig. 13(a), the goodput decreases with the increasing SF at a good underground environment such as VWC equals 10% with Depth equals 0.4 m. This is because the packet loss mainly attributes to the duty cycle restriction, and the growth of airtime caused by the increasing SF reinforces the duty cycle limitations which thus reduces DER_{uplink} (as governed by (10)). However, when the underground environment deteriorates, such as VWC equals 40% and Depth is 0.8 m, the goodput sharply increases to 7.76 bps as SF increases from 7 to 10, before dropping to 7.36 bps with SF being further increased from 10 to 12. In the first stage, the grown SF causes the increase in the link quality, thereby leads to the increase of DER_{uplink} . After the turning point of SF=10 (into the second stage), the increase in SF would lead to an enlarged transmission airtime, which results in reinforced duty cycle restrictions and the increased probability of collision between packets. Furthermore, goodput keeps rising with the increasing SF in a poorer environment such as VWC=30% and Depth=1.2 m. In this environment, the loss of packets is mainly due to the path losses and the signal attenuation, therefore, the increase in SF improves the link quality, which increases DER_{uplink} and thus enlarged goodput. Finally, in a challenging deployment environment, e.g., when VWC=40% and Depth =1.3 m, the goodput keeps close to 0.

In contrast to SF, the increase in BW contributes to the growth of the goodput at a good deployment environment. Because a bigger BW means a shorter airtime of the transmission, it loosens the duty cycle limitation which means more packets can be transmitted. As a result, DER_{uplink} can be increased, hence the goodput (as governed by (10)). On the other hand, for a poor environment, similar trends are observed in Fig. 12(b) and Fig. 13(b), where the goodput keeps decreasing with the increasing BW. In this case, the packet loss is mainly due to the path

losses and the signal attenuation.

As shown in Fig. 13(c), the increase in TP doesn't affect the goodput under good underground environmental conditions, which is similar to Fig. 12(c). That is because a small transmission power can meet the network requirement so that DER_{uplink} keep stable with the increase in TP, which leads to the goodput maintain unchanged. However, although increasing TP will be able to help enlarge the goodput at the GW, it still inevitably cannot reach high goodput for challenging underground environments.

Battery replacement is a much more of issue for WUSNs applications compared to WSNs. It is therefore advisable to more efficiently control the network energy consumption (NEC) through optimizing the physical layer parameters. Therefore, we evaluated the impact of physical layer parameters on NEC, as expressed in Fig. 14.

In Fig. 14(a), NEC increases with the increasing SF due to the increased transmission duration. Except for SF=12, NEC does not vary with underground environments. However, at SF=12, NEC in a good underground environment (e.g., VWC=10% and Depth=0.4 m) is less than that in a poor underground environment (e.g., VWC=40% and Depth=1.2 m). This is because the increasing number of retransmissions leads to the increase of NEC in the poor environment. Contrary to SF, NEC decreases as BW increases due to the reduced transmission duration, as displayed in Fig. 14(b). When BW equals 125 kHz, the increased NEC in the poorer underground environment attributes to the increasing number of retransmissions. In Fig. 14(c), the increased current caused by the larger TP leads to more energy consumption [29]. Based on the above results, we find out that a rational selection of physical layer parameters can facilitate the reduction of NEC.

Even though the trends in the impact of physical layer parameters on NEC in various underground environments are similar, the effect of

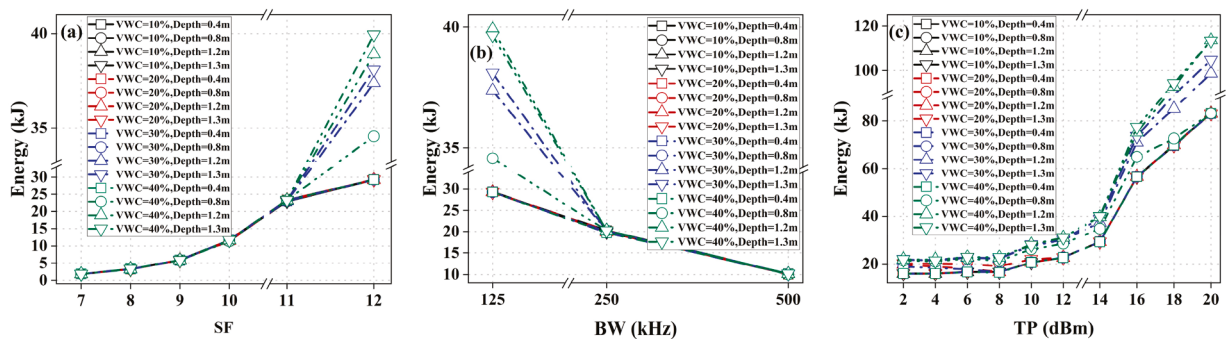


Fig. 14. The impact of (a) SF, (b) BW and (c) TP on the energy for different underground environments.

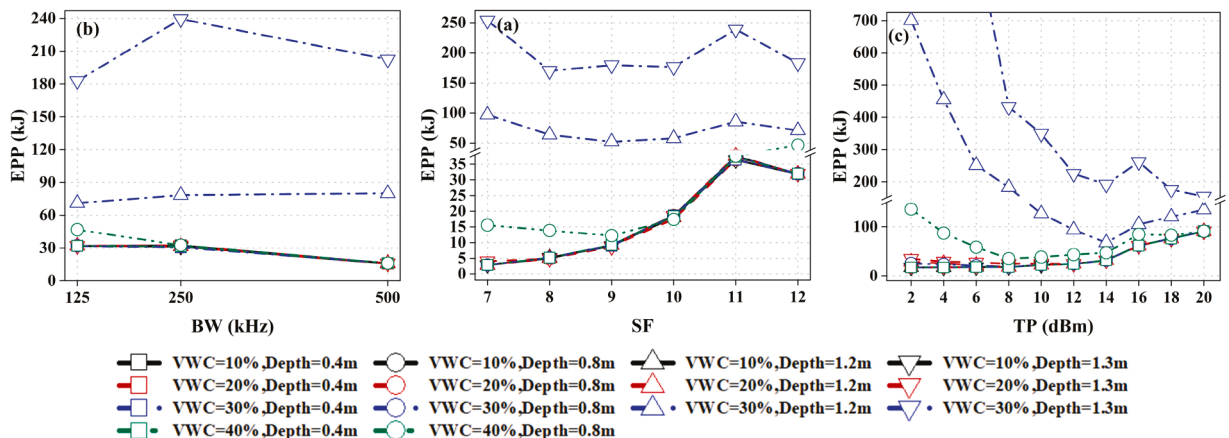


Fig. 15. The impact of (a) SF, (b) BW and (c) TP on the energy per packet for different underground environment.

physical layer parameters on DER varies with different underground environments. Ultimately, one would like to reduce NEC while maintaining a high DER. As a result, we use EPP as an evaluation metric of energy efficiency [34] to capture the trade-off between DER and the consumed energy.

Fig. 15 displays EPP against SF, BW, and TP under various underground environmental conditions. When VWC=40% and Depth>1.2 m, we neglect EPP since it approaches infinity (DER approaching 0). Although NEC rises with the increasing SF as shown in Fig. 14(a), we observe a complex relationship between EPP and SF in Fig. 15(a). For example, the smallest EPP occurs at different SF under different underground environment (i.e., VWC and Depth). Furthermore, it is still worth improving DER by increasing SF even though NEC also rises with the increased SF. For instance, when VWC=10% and Depth=1.2 m, the EPP is reasonably high (EPP=182 kJ) at SF equals 12, where DER reaches 0.92 although the corresponding energy consumption is greater than that of many other SF. Choosing a reasonable SF while sustaining high DER is essential for improving energy efficiency and extending the network lifetime. Besides SF, EPP is also affected by BW. Although DER and NEC decrease with increasing BW as illustrated in Fig. 12(b) and Fig. 14(b), respectively, EPP depends on the ratio of NEC and DER. As seen in Fig. 15(b), EPP shows non-linear variation with increasing BW under different underground environmental conditions. For instance, the maximum EPP occurs when BW equals 250 kHz when VWC=30% and Depth=1.3 m. In this case, by choosing other BW, EPP can be much smaller. Fig. 15(c) shows the impact of TP on EPP. It is observed that the increase in TP leads to poorer energy efficiency (higher EPP) under good underground environmental conditions, since the increased TP has little effect in enhancing DER (Fig. 12(c)), while it can significantly enlarge the energy consumption (Fig. 14(c)). On the contrary, the energy efficiency can increase with the grown TP at the poor environmental conditions because the increase TP can greatly enhance DER. How to reasonably adjust or tune the physical layer parameters to improve the network energy efficiency while sustaining high DER is a crucial problem. This is especially important for WUSNs with different underground environments, and the optimization of the energy consumption through the physical layer parameters shall be further investigated in the future.

6. Conclusion

The monitoring of the underground environment and underground infrastructure becomes more and more essential for exploiting the underground. In this paper, we propose to utilize the LoRaWAN-based WUSNs technology to accomplish such a task. Our comprehensive feasibility analysis starts with our network simulator specifically designed for the LoRaWAN-based WUSNs with bi-directional communication capability. The simulation results successfully validate that it is indeed feasible to use the LoRaWAN-based WUSNs technology for the continuous and extensive observation of the underground environment. It proves to be a much more suitable technology than traditional WSNs or WUSNs technologies. However, the complex underground environment serves a critical influencer for the performance of this technology. For instance, for the better network performance, we prefer to have no more than 1300 nodes in a circle range of less than 6 km in radius if the sensor is buried at 0.1 m with VWC=10%. Larger burial depth or VWC would further restrict the communications range to hundreds of or tens of meters. Finally, a reasonable selection of the physical layer parameters is conducive to enhancing the performance of LoRaWAN-based WUSNs thereby improving the data reception accuracy and observation lifetime. We find that, unlike the WSN's stability in air, the impact of physical layer parameters on the network performance is heavily influenced by the subsurface environment, and that this influence is complex. When choosing physical layer parameters for different underground environments, it is crucial to consider DER, goodput, and energy efficiency, where a trade-off between them must be carefully determined. For instance, the impacts of SF, BW and TP on EPP exhibit

volatility. The selection of physical layer parameters should consider not only the communication characteristics but also the characteristics of the underground environment.

In the future, utilizing this simulator, LoRaWAN-based WUSNs in different underground scenarios shall be investigated. Furthermore, efforts shall be put on how to effectively improve the LoRaWAN-based WUSNs communication performance and energy efficiency by adjusting transmission configurations, through the design of more advanced network architectures or with the aid of machine learning.

Declaration of Competing Interest

The authors declare that they have no known competing financial interests or personal relationships that could have appeared to influence the work reported in this paper.

Data availability

Data will be made available on request.

Acknowledgement

This work was supported by the National Natural Science Foundation of China under Grants No. 42074179, and No. 42211530077.

References

- [1] I. Shahrou, H. Bian, X. Xie, Z. Zhang, Smart technology applications for the optimal management of underground facilities, *Underground Space* 6 (2021) 551–559.
- [2] E. Chuvieco, *Earth Observation of Global change: The role of Satellite Remote Sensing in Monitoring the Global Environment*, Springer, 2008.
- [3] X. Zheng, Z. Feng, H. Xu, Y. Sun, Y. Bai, B. Li, L. Li, X. Zhao, R. Zhang, T. Jiang, X. Li, X. Li, Performance of four passive microwave soil moisture products in maize cultivation areas of Northeast China, *IEEE J. Selected Topics in Appl. Earth Observ. Remote Sens.* 13 (2020) 2451–2460.
- [4] C. Ye, Y. Li, P. Cui, L. Liang, S. Pirasteh, J. Marcato, W.N. Gonçalves, J. Li, Landslide detection of hyperspectral remote sensing data based on deep learning with constraints, *IEEE J. Selected Topics in Appl. Earth Observ. Remote Sens.* 12 (2019) 5047–5060.
- [5] I.F. Akyildiz, E.P. Stuntebeck, Wireless underground sensor networks: research challenges, *Ad Hoc Netw.* 4 (2006) 669–686.
- [6] M.C. Vuran, A. Salam, R. Wong, S. Irmak, Internet of underground things in precision agriculture: architecture and technology aspects, *Ad Hoc Netw.* 81 (2018) 160–173.
- [7] M.E. Bayrakdar, A smart insect pest detection technique with qualified underground wireless sensor nodes for precision agriculture, *IEEE Sens. J.* 19 (2019) 10892–10897.
- [8] D. Abdorahimi, A.M. Sadeghioon, Comparison of radio frequency path loss models in soil for wireless underground sensor networks, *J. Sensor Actuator Networks* 8 (2019).
- [9] F.K. Banaseka, F. Katsriku, J.D. Abdulai, K.S. Adu-Manu, F.N.A. Engmann, Signal propagation models in soil medium for the study of wireless underground sensor networks: a review of current trends, *Wireless Commun. Mobile Comput.* 2021 (2021), 8836426.
- [10] M.E. Bayrakdar, Rule based collector station selection scheme for lossless data transmission in underground sensor networks, *China Commun.* 16 (2019) 72–83.
- [11] M. Tay, A. Senturk, A New Energy-Aware Cluster Head Selection Algorithm for Wireless Sensor Networks, *Wireless Personal Commun.* 122 (2022) 2235–2251.
- [12] S. Wu, A.C.M. Austin, A. Ivoghlian, A. Bisht, K.I.K. Wang, Long range wide area network for agricultural wireless underground sensor networks, *J. Ambient Intell. Humaniz. Comput.* (2020).
- [13] K. Lin, T. Hao, Z. Yu, W. Zheng, W. He, A Preliminary Study of UG2AG Link Quality in LoRa-based Wireless Underground Sensor Networks, in: 2019 IEEE 44th Conference on Local Computer Networks (LCN), 2019, pp. 51–59.
- [14] U. Raza, P. Kulkarni, M. Sooriyabandara, Low Power Wide Area Networks: an Overview, *IEEE Commun. Surveys Tutorials* 19 (2017) 855–873.
- [15] F.K. Banaseka, H. Franklin, F.A. Katsriku, J.-D. Abdulai, A. Ekpezu, I. Wiafe, Soil medium electromagnetic scattering model for the study of wireless underground sensor networks, *Wireless Commun. Mobile Comput.* 2021 (2021), 8842508.
- [16] D.W. Sambo, A. Forster, B.O. Yenke, I. Sarr, B. Gueye, P. Dayang, Wireless Underground Sensor Networks Path Loss Model for Precision Agriculture (WUSN-PLM), *IEEE Sens. J.* 20 (2020) 5298–5313.
- [17] X. Wan, Y. Yang, J. Cui, M.S. Sardar, Lora propagation testing in soil for wireless underground sensor networks, in: 2017 Sixth Asia-Pacific Conference on Antennas and Propagation (APCAP), 2017, pp. 1–3.

- [18] M.C. Bor, U. Roedig, T. Voigt, J.M. Alonso, Do LoRa low-power wide-area networks scale?, in: Proceedings of the 19th ACM International Conference on Modeling, Analysis and Simulation of Wireless and Mobile Systems, 2016, pp. 59–67.
- [19] Z. Sun, I.F. Akyildiz, G.P. Hancke, Dynamic Connectivity in Wireless Underground Sensor Networks, *IEEE Trans. Wireless Commun.* 10 (2011) 4334–4344.
- [20] B. Silva, R.M. Fisher, A. Kumar, G.P. Hancke, Experimental Link Quality Characterization of Wireless Sensor Networks for Underground Monitoring, *IEEE Trans. Industrial Inform.* 11 (2015) 1099–1110.
- [21] M. Capuzzo, D. Magrin, A. Zanella, Mathematical Modeling of LoRa WAN Performance with Bi-directional Traffic, in: 2018 IEEE Global Communications Conference (GLOBECOM), 2018, pp. 206–212.
- [22] M. Capuzzo, D. Magrin, A. Zanella, Confirmed traffic in LoRaWAN: pitfalls and countermeasures, in: 2018 17th Annual Mediterranean Ad Hoc Networking Workshop (Med-Hoc-Net), 2018, pp. 1–7.
- [23] H. Lee, K. Ke, Monitoring of Large-Area IoT Sensors Using a LoRa Wireless Mesh Network System: design and Evaluation, *IEEE Trans. Instrum. Meas.* 67 (2018) 2177–2187.
- [24] K. Mikhaylov, P. Juha, T. Haenninen, Analysis of Capacity and Scalability of the LoRa Low Power Wide Area Network Technology, in: European Wireless 2016; 22th European Wireless Conference, 2016, pp. 1–6.
- [25] F.V.d. Abeele, J. Haxhibeqiri, I. Moerman, J. Hoebeke, Scalability Analysis of Large-Scale LoRaWAN Networks in ns-3, *IEEE Internet of Things J.* 4 (2017) 2186–2198.
- [26] D. Magrin, M. Capuzzo, A. Zanella, A Thorough Study of LoRaWAN Performance Under Different Parameter Settings, *IEEE Internet of Things J.* 7 (2020) 116–127.
- [27] C. Bouras, V. Kokkinos, N. Papachristos, Performance evaluation of LoraWan physical layer integration on IoT devices, in: 2018 Global Information Infrastructure and Networking Symposium (GIIS), 2018, pp. 1–4.
- [28] L. Alliance, A technical overview of LoRa and LoRaWAN, white paper, November 20 (2015).
- [29] N. Sornin, M. Luis, T. Eirich, T. Kramp, O. Hersent, Lorawan Specification, LoRa alliance, 2015.
- [30] K. Lin, T. Hao, Experimental link quality analysis for LoRa-based wireless underground sensor networks, *IEEE Internet of Things J.* 8 (2021) 6565–6577.
- [31] R.W. King, M. Owens, T.T. Wu, Lateral Electromagnetic waves: Theory and Applications to communications, Geophysical exploration, and Remote Sensing, Springer Science & Business Media, 2012.
- [32] V.L. Mironov, L.G. Kosolapova, S.V. Fomin, Physically and mineralogically based spectroscopic dielectric model for moist soils, *IEEE Trans. Geosci. Remote Sensing* 47 (2009) 2059–2070.
- [33] K. Lin, T. Hao, Link quality analysis of wireless sensor networks for underground infrastructure monitoring: a non-backfilled scenario, *IEEE Sens. J.* 21 (2021) 7006–7014.
- [34] J. Park, K. Park, H. Bae, C.K. Kim, EARN: enhanced ADR with coding rate adaptation in LoRaWAN, *IEEE Internet of Things J.* 7 (2020) 11873–11883.
- [35] M. Nurgaliyev, A. Sayimbetov, Y. Yashchyshyn, N. Kuttybay, D. Tukymbekov, Prediction of energy consumption for LoRa based wireless sensors network, *Wireless Networks* 26 (2020) 3507–3520.
- [36] SX1272 LoRa Calculator, <https://www.semtech.com/products/wireless-rf/lora-connect/sx1272> (accessed on 7th Dec. 2022).
- [37] N. Jaja, Understanding the texture of your soil for agricultural productivity, (2016).
- [38] A. Pop, U. Raza, P. Kulkarni, M. Sooriyabandara, Does bidirectional traffic do more harm than good in LoRaWAN Based LPWA networks?, in: GLOBECOM 2017 - 2017 IEEE Global Communications Conference, 2017, pp. 1–6.
- [39] M. Knight, B. Seeber, Decoding LoRa: realizing a modern LPWAN with SDR, in: Proceedings of the GNU Radio Conference, 2016.
- [40] M. Hardie, D. Hoyle, Underground wireless data transmission using 433-MHz LoRa for agriculture, *Sensors* 19 (2019).



Guozheng Zhao received the BSc degree from Shandong University of Science and Technology, Qingdao, China, in 2019. He is currently pursuing an MEng degree with the College of Surveying and Geo-informatics, Tongji University, Shanghai, China. His current research interests include wireless underground sensor networks, low-power wide-area networks, reinforcement learning, and underground environment monitoring.



Kaiqiang Lin received the BEng degree from Fujian Agriculture and Forestry University, Fujian, China, in 2018. He is currently pursuing the PhD degree with the College of Surveying and Geo-Informatics, Tongji University, Shanghai, China. Since November 2021, he is also a visiting PhD student in the center for Wireless Communications (CWC), University of Oulu (UO). His current research interests include Internet of Underground Things, LoRaWAN, and Underground Monitoring.



Tong Hao received the BSc degree from Nanjing University, Nanjing, China, in 2003, the MPhil degree in electronic and electrical engineering from the University of Bath, Bath, U.K., in 2004, and the DPhil degree in engineering science from the University of Oxford, Oxford, U.K., in 2009. From 2010 to 2011, he was a Postdoctoral Research Fellow with the University of Birmingham, Birmingham, U.K. From 2012 to 2014, he was a Specialist with the Oil and Gas Sector, General Electric Company, Farnborough, U.K. He is currently a Professor with the College of Surveying and Geo-Informatics, Tongji University, Shanghai, China. His current research interests include nondestructive testing using electromagnetic and acoustic technologies, RFID, enhanced detection, and sensing of buried infrastructure.